DOI: 10.1002/chem.201002385

A General Strategy for the Preparation of Hollow Carbon Nanocages by NH_4Cl-Assisted Low-Temperature Heat Treatment

Shang Jun Teng,[a, b] Jian Nong Wang,*[b] Bao Yu Xia,[a] and Xiao Xia Wang[c]

Nanostructured graphitic carbon materials have well-developed crystalline structures, high electrical conductivity, good thermal stability, and oxidation resistance at low temperature.[1–4] As a result they have potential applications in many fields as adsorbents, energy storage media, catalyst supports, and electrode materials. Particularly, it has been proposed that such materials can lead to a higher electrocatalytic activity and improved durability when used as a catalyst support compared with conventional amorphous carbon.[5–7] Carbon nanocages (CNCs) have a special hollow structure with graphitic shells and show excellent performance as a catalyst support in proton exchange membrane fuel cells (PEMFC).[8–11]

To date, some methods have been developed to prepare CNCs.[8,9,12–15] Chemical vapor deposition (CVD) is a widely employed technique due to its simplicity and high yield. This method involves the catalytic decomposition of molecules containing carbon atoms. The catalyst is generally a transition metal (e.g., Fe) and the metal forms the core for the formation of external graphitic shells. To obtain hollow CNCs, it is necessary to remove the encapsulated metal particles.

[a] S. J. Teng, B. Y. Xia
Shanghai Key Laboratory for Laser Processing and Materials Modification, School of Materials Science and Engineering, Shanghai Jiao Tong University
800 Dong Chuan Road, Shanghai 200240 (P.R. China)

[b] S. J. Teng, Prof. J. N. Wang
Key Laboratory of Safety Science of Pressurized Systems, (Ministry of Education)
School of Mechanical and Power Engineering
East China University of Science and Technology
130 Meilong Road, Shanghai 200237 (P.R. China)
Fax: (+86) 21-6425-2360
E-mail: jnwang@ecust.edu.cn

[c] Dr. X. X. Wang
School of Materials Science and Engineering, Tongji University
1239 Siping Road, Shanghai 200092 (P.R. China)

Supporting information for this article is available on the WWW under http://dx.doi.org/10.1002/chem.201002385.

At present, little attention has been paid to the removal of the metal particles encapsulated in the CNCs. Boiling in concentrated acid (HNO_3, H_2SO_4, HCl, etc.) is a generally used method.[13,16–20] But these acids have strong oxidation effects, which damage the graphitic structure and also cause a significant loss of carbon material. In addition, strong acids are not desirable for large-scale production because of high costs and environmental concerns.[16–18,21–23] Furthermore, when CNCs are prepared at high temperature by CVD, they have a well-developed and thick graphitic structure, and thus the trapped metal particles cannot be removed because of the high resistance of the graphitic shells to acid oxidation.[21–27]

In this study, we report a simple and low cost method for the preparation of hollow CNCs. First, iron/graphite core–shell nanoparticles are produced by pyrolysis of a mixture of acetylene and iron carbonyl. Then, the core–shell nanoparticles are heat treated in the range of 300–500 °C in the presence of a very cheap chemical, namely, NH_4Cl. Finally, they are mixed with water and filtered. As will be shown, the Fe particles trapped by graphitic shells can be removed with little damage to the graphitic structure and with minimal loss of the carbon material. The possible mechanism will also be discussed. The hollow CNCs thus obtained are demonstrated to show improved electrochemical catalytic activity when used as a support material for Pt than CNCs obtained by acid processes.

The as-prepared samples of iron/graphite core–shell nanoparticles formed as a black powder and the XRD pattern is illustrated in Figure 1a. The peak at $2\theta = 26.1°$ could be attributed to diffraction from the (002) planes of the hexagonal structure of graphite. The highest peak appearing at $2\theta = 44.9°$ could be attributed to the diffraction of the (110) plane of Fe, the (031) plane of Fe_3C, and the (101) plane of graphite. The rest of the peaks are related to Fe_3C. A TEM image of the sample is shown in Figure 1b. As can be seen, the as-prepared particles have sizes in the range of 30–50 nm. Furthermore, each nanoparticle has an iron/graphite core–shell structure (inset in Figure 1b). The thickness of the shell of the particle is about 4–8 nm.

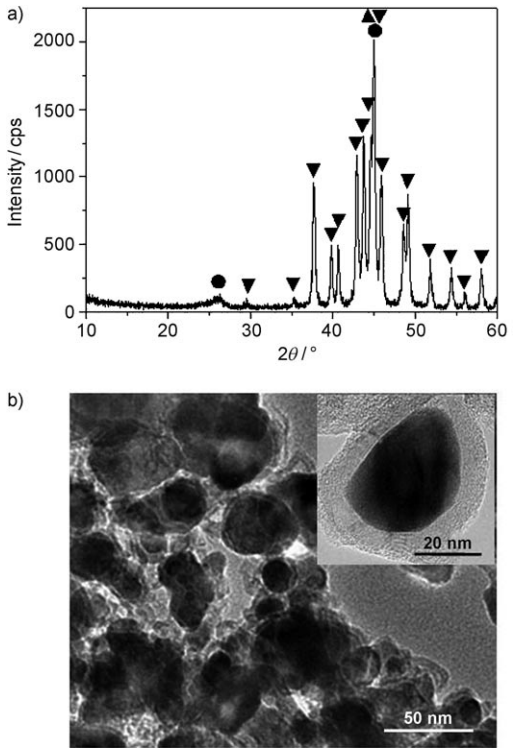

Figure 1. XRD pattern (a) and TEM image (b) of the as-prepared sample; ● = C, ▲ = Fe, ▼ = Fe_3C.

After heat treatments with NH_4Cl, the samples were examined by XRD (Figure 2). As can be seen in Figure 2a, the peaks for $(NH_4)_3FeCl_5$ appeared after heat treatment at 300 °C in addition to the diffraction peaks for NH_4Cl. After being filtered with water, $(NH_4)_3FeCl_5$ and NH_4Cl disappeared and only graphitic carbon remained. After heat treatment at 400 °C, as can be seen in Figure 2b, NH_4FeCl_3 rather than $(NH_4)_3FeCl_5$ formed and the intensities of the peaks corresponding to NH_4Cl became weaker than those at 300 °C, suggesting a lower amount of NH_4Cl in the final product. After filtration with water, NH_4FeCl_3 and NH_4Cl disappeared and only graphitic carbon remained. When the heat treatment temperature was increased to 500 or 600 °C, the original NH_4Cl could no longer be observed and instead $FeCl_2$ and $FeCl_2{\cdot}2H_2O$ were observed, as shown in Figure 2c and d. After filtration with water, $FeCl_2$ and $FeCl_2{\cdot}2H_2O$ disappeared and there was only graphitic carbon in the sample. These results indicate that NH_4Cl-assisted low-temperature heat treatment is an effective method to remove the Fe particles trapped by well-developed graphitic shells.

Figure 3 shows the TEM images of the sample after NH_4Cl treatment at 400 °C and filtration with water. The TEM image shows that the Fe particles have been removed completely. The size of the hollow cages is 30–50 nm for the outer diameter with the shell thickness being 4–8 nm (Figure 3a), which is consistent with the as-prepared sample. HRTEM illustrates that the cage shell is composed of well-

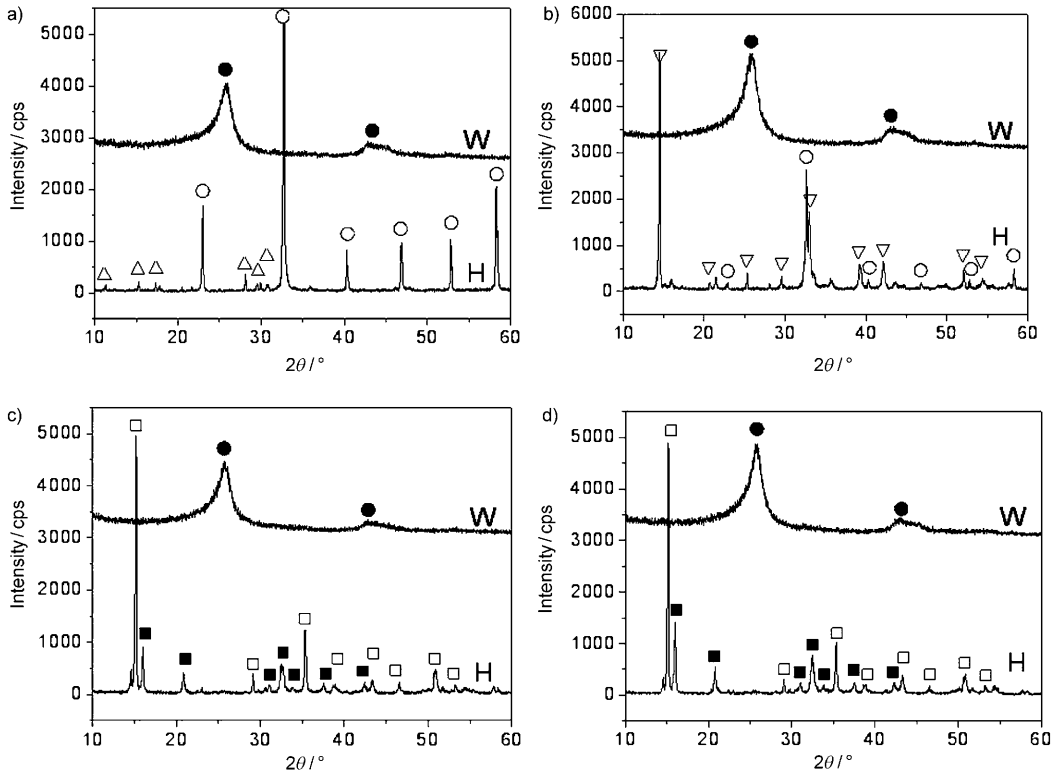

Figure 2. XRD patterns of CNC samples after heat-treatment with NH_4Cl (marked H) and after further filtration in water (marked W): a) 300, b) 400, c) 500, d) 600 °C; ● = C, ○ = NH_4Cl, △ = $(NH_4)_3FeCl_5$, ▽ = NH_4FeCl_3, □ = $FeCl_2$, ■ = $FeCl_2{\cdot}2H_2O$.

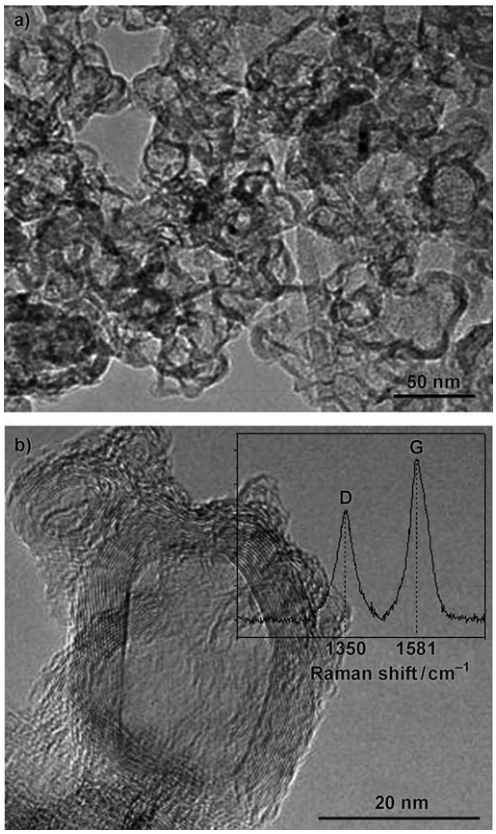

Figure 3. TEM image (a) and HRTEM image (b) of CNCs after heat-treatment at 400 °C for 1 h with NH_4Cl and further filtering in water. The inset shows the Raman spectrum of the CNCs.

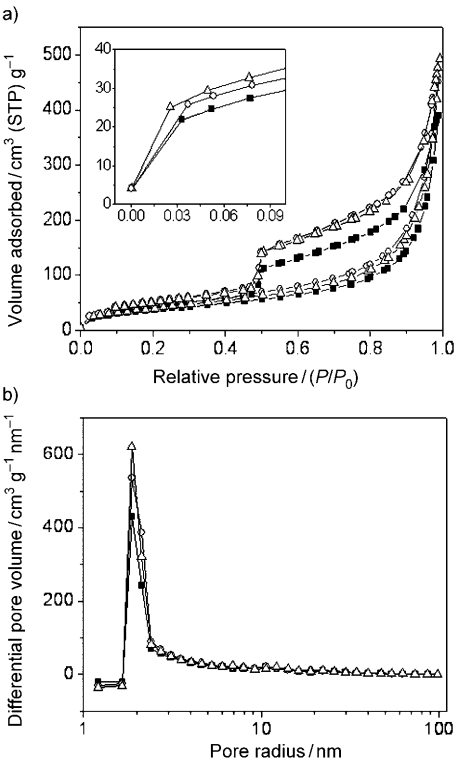

Figure 4. N_2 adsorption/desorption isotherms and enlarged N_2 adsorption isotherms at low partial pressure ($P/P_0 < 0.3$) (a), mesopore size distribution (b) of the CNCs after heat treatments with NH_4Cl at different temperatures and further filtering; ■ = 300, ○ = 400, △ = 500 °C.

defined graphitic layers with a spacing of 0.34 nm (Figure 3b).

The graphitization of the present hollow CNCs can be further characterized by Raman spectroscopy as shown in the inset of Figure 3b. The spectrum of the CNCs shows two peaks characteristic of the graphite structure at approximately 1350 and 1581 cm^{-1}, respectively. The peak at 1581 cm^{-1} can be identified as the G peak of the perfect crystalline graphite arising from the zone-center E_{2g} mode, and the peak at 1350 cm^{-1} as the D peak assigned to the A_{1g} zone-edge phonon induced by the disorder in the graphite lattice.[24–27] The ratio of the integrated intensities of G and D bands (IG/ID = 1.50) of the CNCs indicates that the graphitization of the present hollow CNCs remained quite good after heat treatment at 400 °C.

N_2 adsorption/desorption experiments were carried out to analyze the pore structures of CNCs obtained by NH_4Cl treatment (Figure 4). The measurements showed that the CNCs heat treated at 300, 400, and 500 °C had a specific surface area S_{BET} of 137, 164, and 150 m^2 g^{-1}, respectively. As shown in Figure 4a, the CNC samples exhibit typical IV isotherms with H1 hysteresis.[28–29] The obvious hysteresis of desorption for CNCs from NH_4Cl treatment between the partial pressures P/P_0 of 0.5 and 1.0 suggests the existence of predominant mesopores.[30] At low pressures ($P/P_0 < 0.3$), the uptake for the sample resulting from NH_4Cl treatment demonstrates the existence of more micropores (inset in Figure 4a, the enlarged adsorption isotherms). The mesopore size distributions determined by the Barrett–Joyner–Halenda (BJH) method are shown in Figure 4b. The mesopore size distributions are similar for different samples (Figure 4b), but the pore volumes of the 400 and 500 °C samples are slightly larger than the 300 °C one. The reason for this difference might be that iron particles could be removed more completely when treated at higher temperatures. Measurements showed that acid treatment induced more mesopores in the CNCs than the NH_4Cl treatment (see Figure S1 in the Supporting Information).

To investigate the performance of the present hollow CNCs as a catalyst support, the CNCs from the heat treatment at 400 °C were taken as an example. An electrochemical study of the Pt catalyst (45 wt %, based on theoretical calculation and determined by thermogravimetry analysis) supported on CNCs (Pt/CNC (NH_4Cl)) was performed. For comparison, the catalyst supported on CNCs from acid treatment (Pt/CNC (acid)) according to the method reported in our previous publication[31] and the catalyst supported on conventional carbon black (Pt/CB, 45 wt %) were also prepared by the same process.

Figure 5a shows the XRD pattern and a typical TEM micrograph of the catalyst formed of Pt/CNC (also see Figure S2 in the Supporting Information). Pt particles are finely and uniformly dispersed on the CNCs. Statistical estimation

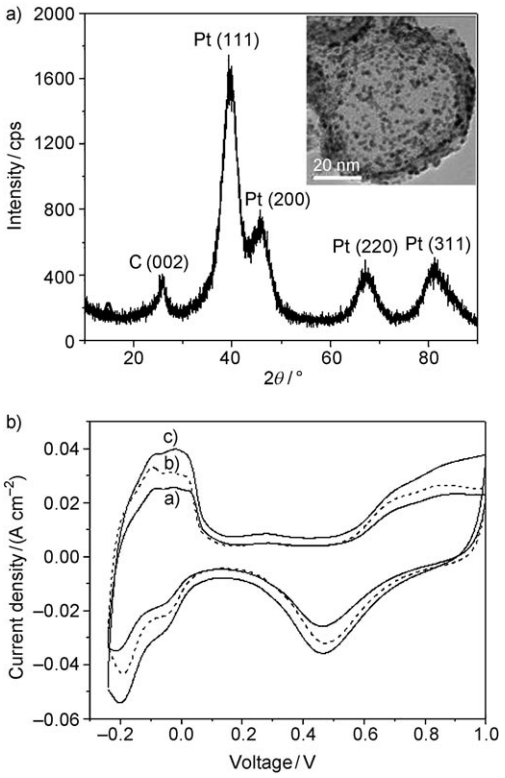

Figure 5. XRD pattern and TEM image of Pt/CNC catalyst (a), cyclic voltammograms of different catalysts (b); a) Pt/CB, b) Pt/CNC (acid), and c) Pt/CNC (NH_4Cl) (scanning rate 100 $mV\,s^{-1}$).

reveals that the average size of the Pt particles on the support is about 3.0 nm. The mean size of the Pt particles can also be calculated from the Pt (220) peak of the XRD lines (Figure 5b) according to Scherrer's formula.[27] The value determined from XRD is slightly less than 3.0 nm, in close agreement with that from the TEM image.

Figure 5b shows the cyclic voltammograms of the different catalysts using different supports, Pt/CB, Pt/CNC (acid), and Pt/CNC (NH_4Cl). As can be seen, the catalyst Pt/CNC (NH_4Cl) demonstrates stronger hydrogen desorption and adsorption peaks and thus a higher electroactivity than other two catalysts.

The electroactive surface area for a catalyst can be estimated from the following equation: $\alpha = Q/(m \times \beta)$, in which Q is the charge of hydrogen desorption, m is the quantity of Pt used, and β is the charge required to oxidize a monolayer of H_2 on bright Pt (assumed to be 210 $\mu C\,cm^{-2}$). The Q value can be calculated from a cyclic voltammogram without taking into account the contribution of the charge from the electric double layer. The results presented in Table 1 show

Table 1. Coulombic charge for hydrogen desorption (Q) and electroactive surface area (α) calculated for different catalysts.

Catalyst	Q [$mC\,cm^{-2}$]	α [$m^2\,g^{-1}$]
Pt/CB	44.20	52.62
Pt/CNC (acid)	57.50	68.45
Pt/CNC (NH_4Cl)	64.80	81.43

that α for the Pt/CNC (NH_4Cl) catalyst is clearly higher than the Pt/CB and Pt/CNC (acid) catalysts.

The present results expressly reveal that NH_4Cl-assisted low-temperature heat treatment is an effective method to remove the metal particles trapped in core–shell nanoparticles. The formation of this core/shell structure may be related to the activities of the carbon source and metal particles. At high temperature, the decomposition of $Fe(CO)_5$ yielded iron nanoparticles that possessed a very high catalytic activity for the decomposition of C_2H_2. The decomposed carbon was dissolved in iron particles. When the temperature decreased, carbon would become oversaturated, precipitate, and then deposit on the surfaces of the iron particles. Consequently, iron/graphite core–shell nanoparticles with graphitic layers formed.

To get hollow CNCs, the iron particles need to be removed. When iron/graphite core–shell nanoparticles were boiled in acid, the trapped iron particles could be removed at the expense of destroying the graphite layers. The compact graphitic shells were first opened at their amorphous regions by selective oxidation of nitric acid, and then the iron particles were dissolved by acid through the opened channels.[13]

When the core–shell nanoparticles were heat treated at low temperature in the presence of NH_4Cl, the iron particles could be removed completely without damage to graphitic shells during heat treatment. This may be due to the fact that there is no reaction, including N doping, between graphitic carbon and NH_4Cl during heat treatment (Figure S3 in the Supporting Information). Therefore, the mechanism for the removal of iron particles by NH_4Cl treatment is different from that of acid treatment and could be related to the diffusion of iron particles.

Two types of diffusion may occur during heat treatment, including the inward diffusion of NH_4Cl along the graphitic shells and outward diffusion of Fe. The inward diffusion of NH_4Cl is unlikely because there is no reaction space available in the core. If a reaction occurred in the core, the volume of the core would increase. Thus, the graphitic shell would exert a pressure on the core and this pressure would hinder further reaction. To continue the reaction, the reaction product needs to diffuse out from the core, but this would hinder the inward diffusion of NH_4Cl. For these reasons the inward diffusion of NH_4Cl could hardly occur.

The outward diffusion of Fe may be the main type of diffusion during the removal of iron particles and this was also observed by other researchers.[32] To promote the outward diffusion of iron nanoparticles, there must be a driving force; one suggestion was particle melting.[33] It has been reported that iron nanoparticles become unstable when heated even at 250 °C.[34] When heated above this temperature, the original iron particle in the core could have a high activity and as such have a tendency to cause outward diffusion. The micropores/mesopores and defects existing in CNCs may provide a facility for the outward diffusion of Fe atoms to enable the reaction with NH_4Cl.

Due to its low sublimation point (≈350 °C), NH_4Cl would begin to evaporate at 300 °C and become completely gaseous at 400 °C. At these temperatures, NH_4Cl could still exist in the molecular form. When Fe atoms have escaped from the CNCs, they could react immediately with NH_4Cl existing in the environment. Thus, $(NH_4)_3FeCl_5$ is formed at 300 °C and NH_4FeCl_3 at 400 °C. When heated to 500 °C and above, NH_4Cl would completely decompose to NH_3 and HCl. Therefore, the Fe reacts with HCl to form $FeCl_2$. Since NH_4Cl, $(NH_4)_3FeCl_5$, NH_4FeCl_3, and $FeCl_2$ dissolve in water, they can easily be removed from the heated samples.

As a support for Pt nanoparticles, the hollow CNCs from NH_4Cl treatment perform better than hollow CNCs obtained by acid treatment. The main reason for this may be that CNCs from NH_4Cl treatment have a better graphitic structure and thus a better conductivity than the acid-treated counterpart. In the present process, the iron particles were removed by outward diffusion of Fe atoms through micropores/mesopores or defects existing in CNCs when heated at low temperature. Therefore, the original graphitic structure could be preserved with little damage. In addition to the application as a catalyst support, the present CNCs could have many other applications in many areas, such as adsorbents, electrode materials, and energy-storage media because they have a unique dimension and structure.[35–40]

In conclusion, a simple method was developed for the preparation of hollow CNCs. First, iron/graphite core–shell nanoparticles with good graphitization were synthesized by pyrolysis of acetylene with iron carbonyl. Then, the nanoparticles were heat treated at low temperature in the presence of NH_4Cl and filtered with water. It was found that the iron particles could be completely removed and hollow CNCs with good graphitization could be obtained. The mechanism for removal of iron particles may be that Fe atoms diffuse out from CNCs and react with NH_4Cl or its decomposition product of HCl. When the hollow CNCs were used as a support material for Pt nanoparticles, the Pt/CNC catalyst showed apparent improvement in electrochemical activity. Therefore, the present method could be applied to the production of graphitic carbon on a large scale. And the resultant CNCs could prove to be practically relevant for fuel cells and many other technologies.

Experimental Section

Preparation of core–shell nanoparticles: The iron/graphite core–shell nanoparticles were prepared by a CVD approach. N_2/C_2H_2 mixed gases were flowed through the liquid iron carbonyl ($Fe(CO)_5$) into a quartz reactor heated at 1000 °C. N_2 was used as a carrier gas at a flow rate of 140 L h^{-1} and C_2H_2 as the carbon source at 60 mL min^{-1}. The prepared sample was collected in a glass bottle connected to the quartz reactor.

Removal of the metal core: The as-prepared sample was mixed with excess NH_4Cl and placed at one end of a quartz tube. The tube was evacuated and filled with N_2 to atmospheric pressure. The heat treatments were carried out at temperatures of 300–600 °C for 60 min. After cooling to ambient temperature, the heated sample was directly washed with water and filtered. The sample collected on the filter was dried at 80 °C for 3 h. For the purpose of comparison, the as-prepared sample was also refluxed in a mixed acid solution of HCl and HNO_3 with a volume ratio of 3:1 at 120 °C for 6 h. The solution was diluted with distilled water, and similarly filtered, washed, and dried.

Characterization of CNCs: The X-ray diffractometer (XRD) was operated at 35 kV and 200 mA with nickel-filtered $Cu_{K\alpha}$ radiation as an incident beam (D/max 2550VL/PC) to study the crystallization of carbon and other phases contained in the samples. Typical transmission electron microscopy (TEM) and high resolution transmission electron microscopy (HRTEM) with a cold field emission gun (JEOL-2010F, accelerating voltage of 200 kV) were used to investigate the microstructure and morphology of the sample. Nitrogen adsorption/desorption isotherms of CNC samples were measured at 77 K using a BELSORP instrument (BEL Inc. Japan). The sample was outgassed at 200 °C under a nitrogen flow for 2 h prior to the measurement. The total surface area was calculated from the Brunauer–Emmett–Teller (BET) equation from the adsorption data at relative pressures from 0.04 to 0.2. The mesopore size distribution (>2 nm) was determined by the Barrett–Joyner–Halenda (BJH) method and the micropore size distribution (<2 nm) was studied by the micropore analysis method (MP method).[27] Raman spectroscopy was carried out to examine the perfection of the hollow CNCs obtained from heat treatment using a Horiba Jobin Yvon HR 800UV with a 514.5 nm excitation wavelength laser.

Preparation of Pt/CNC catalyst and electrochemical activity: Pt/CNC catalysts were prepared by polyol reduction. The amount of Pt deposited was 45 wt% (Figure S4 in the Supporting Information). At first, CNCs were sonicated in ethylene glycol to form a slurry. Then, the slurry was heated up to around 140 °C. A chloroplatinic acid (CPA) solution, prepared by dissolving CPA (H_2PtCl_6) in ethylene glycol, was added slowly into the CNC slurry. The mixture was refluxed at 140 °C for 3 h. After cooling to room temperature, the catalyst was filtered, washed with distilled water, and dried for the subsequent measurement. Glassy carbon (GC) (Bas electrode, 0.07 cm^2) was polished to a mirror with a 0.3 μm alumina powder suspension before each experiment and served as an underlying substrate of the working electrode. To prepare the composite electrode, the Pt/CNC catalyst was dispersed ultrasonically in the mixed solution of ethanol and 5 wt% Nafion solution and a 20 μL aliquot was transferred on to a polished glassy carbon substrate. The amount of Pt on the electrode was controlled to be 0.4 mg cm^{-2} on all electrodes. After the evaporation of ethanol, the resulting thin catalyst film covered the glassy carbon substrate. Then, the electrode was dried at room temperature and used as the working electrode. The electrochemical activities of the catalysts were characterized by cyclic voltammetry (CV). The experiments were performed by using a three-electrode cell with an EG&G potentiostat (Model 366A) at ambient temperature and 0.5 M H_2SO_4 was used as the electrolyte.

Acknowledgements

J.N.W. is thankful to the research fund (project no.: 50871067) from The National Natural Science Foundation of China and the fund for the national 863 projects of 2007AA05Z128 and 2009AA034400 from The Ministry of Science and Technology of China.

Keywords: carbon · fullerenes · mesoporous materials · nanoparticles · platinum

[1] R. Ryoo, S. H. Joo, S. Jun, *J. Phys. Chem. B* **1999**, *103*, 7743–7746.
[2] A.-H. Lu, W. Schmidt, N. Matoussevitch, H. Bönnermann, B. Spliethoff, B. Tesche, E. Bill, W. Kiefer, F. Schuth, *Angew. Chem.* **2004**, *116*, 4403–4406; *Angew. Chem. Int. Ed.* **2004**, *43*, 4303–4306.
[3] B. EI. Hamaoui, L. Zhi, J. Wu, U. Kolb, K. Müllen, *Adv. Mater.* **2005**, *17*, 2957- 2960.

[4] D. Mirabile Gattia, M. V. Antisari, L. Giorgi, R. Marazzi, E. Piscopiello, A. Montone, S. Bellitto, S. Licoccia, E. Traversa, *J. Power Sources* **2009**, *194*, 243–251.
[5] P. V. Shanahan, L. B. Xu, C. D. Liang, M. Waje, S. Dai, Y. S. Yan, *J. Power Sources* **2008**, *185*, 423–427.
[6] D. Bom, R. Andrews, D. Jacques, J. Anthony, B. Chen, M. S. Meier, J. P. Selegue, *Nano Lett.* **2002**, *2*, 615–619.
[7] J. J. Wang, G. P. Yin, Y. Y. Shao, Z. B. Wang, Y. Z. Gao, *J. Phys. Chem. C* **2008**, *112*, 5784–5789.
[8] J. N. Wang, Y. Z. Zhao, J. J. Niu, *J. Mater. Chem.* **2007**, *17*, 2251–2256.
[9] Z. M. Sheng, J. N. Wang, *Adv. Mater.* **2008**, *20*, 1071–1075.
[10] B. Y. Xia, J. N. Wang, X. X. Wang, J. J. Niu, Z. M. Sheng, M. R. Hu, Q. C. Yu, *Adv. Funct. Mater.* **2008**, *18*, 1790–1799.
[11] J. J. Niu, J. N. Wang, L. Zhang, Y. Q. Shi, *J. Phys. Chem. C* **2007**, *111*, 10329–10335.
[12] T. Oku, I. Narita, A. Nishiwaki, *Diamond Relat. Mater.* **2004**, *13*, 1337–1341.
[13] Y. W. Ma, Z. Hu, K. F. Huo, Y. N. Lu, Y. M. Hu, Y. Liu, J. H. Hu, Y. Chen, *Carbon* **2005**, *43*, 1667–1672.
[14] T. Oku, T. Hirano, K. Suganuma, S. Nakajima, *Mater. Res. Soc. Symp. Proc.* **1999**, *14*, 4266–4273.
[15] N. Sano, H. Wang, M. Chhowalla, I. Alexandrou, G. A. J. Amaratunga, *Nature* **2001**, *414*, 506–507.
[16] K. Hernadi, A. Siska, L. Thiên-Nga, L. Forró, I. Kiricsi, *Solid State Ionics* **2001**, *203*, 141–142.
[17] J.-F. Colomer, P. Pierdigrosso, A. Fonseca, J. B. Nagy, *Synth. Met.* **1999**, *103*, 2482–2483.
[18] A. Fonseca, K. Hernadi, J. B. Nagy, D. Bernaerts, A. A. Lucas, *J. Mol. Catal. A* **1996**, *107*, 159–168.
[19] X. C. Chen, C. S. Chen, Q. Chen, F. Q. Cheng, G. Zhang, Z. Z. Chen, *Mater. Lett.* **2002**, *57*, 734–738.
[20] K. Hernadi, A. Fonseca, J. B. Nagy, D. Bernaerts, J. Riga, A. Lucas, *Synth. Met.* **1996**, *77*, 31–34.
[21] M. Holzinger, A. Hirsch, P. Bernier, G. S. Duesberg, M. Burghard, *Appl. Phys. A* **2000**, *70*, 599–602.
[22] T. W. Ebbesen, P. M. Ajayan, H. Hiura, K. Tanigaki, *Nature* **1994**, *367*, 519–519.
[23] A. G. Rinzler, J. Liu, H. Dai, P. Nikolaev, C. B. Huffmann, F. J. Rodriguez-Macias, P. J. Boul, A. H. Lu, D. Heymann, D. T. Colbert, R. S. Lee, J. E. Fisher, A. M. Rao, P. C. Eklund, R. E. Smalley, *Appl. Phys. A* **1998**, *67*, 29–37.
[24] M. Ginic-Markovic, J. G. Matisons, R. Cervini, G. P. Simon, P. M. Fredericks, *Chem. Mater.* **2006**, *18*, 6258–6262.
[25] F. Tuinstra, J. L. Koenig, *J. Chem. Phys.* **1970**, *53*, 1126–1130.
[26] R. J. Nemanich, S. A. Solin, *Phys. Rev .B* **1979**, *20*, 392–401.
[27] V. Radmilovic, H. A. Gasteiger, P. N. Ross, *J. Catal.* **1995**, *154*, 98–106.
[28] S. H. Joo, C. Pak, D. J. You, S. A. Lee, H. I. Lee, J. M. Kim, H. Chang, D. Seung, *Electrochim. Acta* **2006**, *52*, 1618–1626.
[29] S. S. Kim, T. R. Pauly, T. J. Pinnavaia, *Chem. Commun.* **2000**, 1661–1662.
[30] S. J. Gregg, K. S. W. Sing, *Adsorption, in Surface Area and Porosity*, 2nd ed., Academic Press, London, **1982**, pp. 218–228.
[31] S. J. Teng, X. X. Wang, B. Y. Xia, J. N. Wang, *J. Power Sources* **2010**, *195*, 1065–1070.
[32] J. S. Zhou, H. H. Song, X. H. Chen, L. J. Zhi, J. P. Huo, B. Cheng, *Chem. Mater.* **2009**, *21*, 3730–3737.
[33] A. H. Latham, M. J. Wilson, P. Schiffer, M. E. Williams, *J. Am. Chem. Soc.* **2006**, *128*, 12632–12633.
[34] G. Liu, B. X. Qin, Y. B. Guo, R. H. Fan, N. Lu, *Ordnance Mater. Sci. Eng.* **2003**, *360*, 18–22.
[35] R. W. Fu, T. F. Baumann, S. Cronin, G. Dresselhaus, M. S. Dresselhaus, J. H. Satcher, Jr., *Langmuir* **2005**, *21*, 2647–2651.
[36] T. Hyeon, S. Han, Y.-E. Sung, K.-W. Park, Y.-W. Kim, *Angew. Chem.* **2003**, *115*, 4488–4492; *Angew. Chem. Int. Ed.* **2003**, *42*, 4352–4356.
[37] S. Han, Y. Yun, K.-W. Park, Y.-E. Sung, T. Hyeon, *Adv. Mater.* **2003**, *15*, 1922–1925.
[38] A.-H. Lu, W.-C. Li, N. Matoussevitch, B. Spliethoff, H. Bönnermann, F. Schüth, *Chem. Commun.* **2005**, 98–100.
[39] A.-H. Lu, W.-C. Li, E.-L. Salabas, B. Spliethoff, F. Schüth, *Chem. Mater.* **2006**, *18*, 2086–2094.
[40] J. N. Wang, L. Zhang, J. J. Niu, F. Yu, Z. M. Sheng, Y. Z. Zhao, H. Chang, C. Pak, *Chem. Mater.* **2007**, *19*, 453–459.

Received: August 18, 2010
Published online: November 5, 2010

